Catalytic activity of hierarchical beta zeolites in the Prins cyclization of (−)-isopulegol with acetone

Laluc, Mathias; Barakov, Roman; Mäki-Arvela, Päivi; Shcherban, Nataliya; Murzin, Dmitry Yu

Published in:
Applied Catalysis A: General

DOI:
10.1016/j.apcata.2021.118131

Published: 25/05/2021

Document Version
Accepted author manuscript

Catalytic activity of hierarchical beta zeolites in the Prins cyclization of (−)-isopulegol with acetone

Mathias Laluc[a], Roman Barakov[b,c], Päivi Mäki-Arvela[a], Nataliya Shcherban[b], Dmitry Yu. Murzin[a]

[a]*Johan Gadolin Process Chemistry Centre, Faculty of Science and Engineering, Åbo Akademi University, 20500 Turku, Finland,*

e-mail: dmurzin@abo.fi

[b]*L.V. Pisarzhevsky Institute of Physical Chemistry, National Academy of Sciences of Ukraine, 31 pr. Nauky, Kiev, 03028, Ukraine*

[c]*Department of Physical and Macromolecular Chemistry, Faculty of Science, Charles University in Prague, Hlavova 2030, 12840 Prague 2, Czech Republic*

Abstract

Several hierarchical beta zeolites prepared via hydrothermal treatment of a concentrated zeolite gel-precursor were investigated in Prins cyclisation between (–)-isopulegol and acetone acting as a reactant and a solvent for production of a chromenol compound exhibiting antiviral activity. The catalysts were characterized by SEM, TEM, nitrogen physisorption, ammonia TPD, adsorption-desorption of pyridine and 2,4,6-tri-*tert*-butylpyridine with FTIR spectroscopy. For the Prins cyclization performed at 30 °C, the highest yield of the desired product was obtained over a zeolite catalyst containing a developed mesoporosity with a uniform mesopore size and an optimum ratio of Brønsted to Lewis acid sites.

Keywords: hierarchical zeolite, Prins cyclisation, chromenol, tetrahydropyran ring structure

1. Introduction

Application of renewable raw materials, highly active and selective heterogeneous catalysts operating under mild reaction conditions is among the key constituents of the sustainability strategy in chemistry [1,2]. Utilization of natural terpenoids for synthesis of pharmaceuticals allows to obtain different compounds with a 2H-chromene (benzopyran) structure exhibiting anticancer, antiviral, analgesic, fungicidal and other activity [3–5].

Prins cyclization of aldehydes or ketones with alkenes, such as homoallylic ones is typically done over acidic catalysts [6]. The Prins reaction of (−)-isopulegol with aldehydes in the presence of acid catalysts giving octahydro-2*H*-chromen-4-ol (4*R* and 4*S* diastereoisomers), and its dehydration products has been already studied [6–10]. Another interesting and much less explored reaction is (−)-isopulegol cyclization with acetone (Fig. 1). The product, namely the 4*R* isomer of chromenol possesses antiviral properties against H1N1 and H2N2 influenza while the 4*S* diastereomer does not exhibit any anti-virus effect [11].

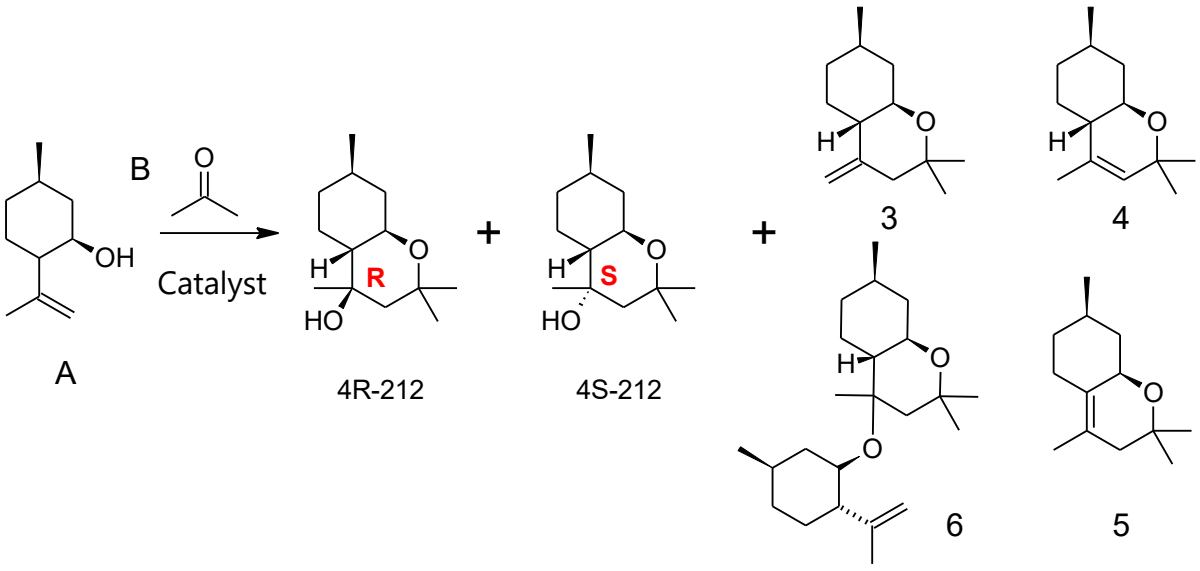

Fig. 1. The reaction scheme for Prins cyclization of (-)-isopulegol (A) with acetone (B) for synthesis of chromenols (4*R* and 4*S* diastereomers)

Synthesis of chromenols using ketones has been scarcely investigated [11,12]. For instance, application of K10 clay as a catalyst resulted in the total yield of chromenols of 21% with the *R*/*S*

ratio of 9:1 [11]. An acid modified K10 clay afforded 57% yield of chromenol with, however, much lower *R*/*S* ratio of only 3:1. Halloysite nanotubes (HNT) pretreated with HCl were discovered to be active catalysts for the Prins reaction with acetone allowing to increase the chromenols yield up to 78% (the *R/S* ratio 8.4) [13]. Condensation of (−)-isopulegol with acetone over large pore K10-clay modified by sulfonic acid allowed the highest yield (73%) of the desired chromenols among the reported ones in the literature [14]. A very limited scope of the tested catalysts and unclear influence of surface acidity and the porous structure prompt evaluation of the effect of acidity and porosity on the catalyst performance.

Hierarchical zeolites contain hierarchically organized pores with at least two levels of porosity: structural micropores and a secondary porosity system, in most cases, mesopores [15]. The presence of mesopores in hierarchical zeolites is beneficial from the viewpoint of diminishing the steric limitations and allowing transformations of bulky molecules exceeding the zeolite micropore size, increasing the diffusion of reactants and products, providing a better dispersion of the active phases, as well as decreasing deactivation by carbon deposition [16–19]. Zeolitic material consisting of a crystalline network of TO_4 tetrahedra that possess, in addition to uniform zeolitic micropores, a secondary porosity, e.g. intracrystalline mesopores betwen zeolite nanoparticles agglomerates, is referred to hierarchical zeolites [20,21]. Due to developed mesoporosity in hierarchical zeolites, promoting accessibility of catalytically active sites for the reactants, and presence of medium strength and strong acid sites [22–25], these materials can be promising catalysts in the Prins cyclization of (–)-isopulegol with acetone. Hierarchical zeolites consisting of beta nanoparticles were obtained via hydrothermal treatment of a concentrated zeolite gel-precursor (H_2O/Si = 2.5 – 14) without utilization of complex structure-directing agents and demonstrated high catalytic activity in the reaction of bulky alcohols (1-octadecanol and 1-adamantanemethanol) with 3,4-dihydro-2*H*-pyran [26]. The textural and acid properties of these materials can be adjusted by changing duration of the hydrothermal treatment (HTT) of the reaction mixture (RM) and H_2O/Si ratio in the starting gel.

The aim of the current work was to investigate the influence of the textural and acidic properties of the obtained hierarchical zeolites on their catalytic activity in the Prins cyclization of (–)-isopulegol with acetone.

2. Experimental part

2.1 Synthesis of the catalysts

Hierarchical beta zeolites (HB – hierarchical beta) were obtained via the thermal treatment of a concentrated beta zeolite reaction mixture (H_2O/Si = 2.5–7.0, Si/Al = 25). Synthesis of the HB samples was carried out using a reaction mixture (RM) with the composition $1SiO_2$: $0.02Al_2O_3$: $0.028Na_2O$: 0.6TEAOH: 0.2HCl: $20H_2O$, with tetraethylammonium hydroxide (TEAOH, 40% aqueous solution, SACHEM, Inc.) as the structure-directing agent. Fumed silica (Aerosil® A-175) and as-synthesized aluminum hydroxide gel (9.8 wt% Al_2O_3) were used as silicon and aluminum sources respectively. Aluminum hydroxide aqueous suspension was prepared by dissolving 10 g $Al(NO_3)\cdot 9H_2O$ (Sigma Aldrich, 98%) in 60 ml of distilled water and increasing pH of the obtained solution to ca. 7 by adding NaOH solution (20 %wt). Then the suspension was washed with water and centrifuged giving $Al(OH)_3$ gel. The content of Al_2O_3 in $Al(OH)_3$ gel was determined by the gravimetric method. The obtained zeolite-forming RM was dried at 75 °C to H_2O/Si molar ratio in the gel 2.5 – 7.0 (Table 1) followed by placing the samples in Teflon liners in an autoclave and hydrothermal treatment (HTT) at 140 °C for 2 – 9 days (samples HB-1 – HB-6). The reference sample of beta zeolite (CB-1 – conventional beta) was obtained by HTT of the zeolite-forming RM (Si/Al = 35) at 140 °C for 7 days without preliminary drying. A detailed procedure for synthesis of HB-1 – HB-6 and CB-1 materials was given previously [26].

Table 1

Synthesis conditions, particle size and degree of crystallinity of the catalysts.

Sample	H_2O/Si molar ratio	τ[a] (days)	Average particle size[b] (nm)	The degree of crystallinity
HB-1	2.5	2	56	0.60
HB-2	2.5	7	45	1.0
HB-3	2.5	9	80	0.75
HB-4	5.5	7	20	0.85
HB-5	7.0	7	23	1.0
HB-6	5.5	9	44	0.60
CB-1	20	7	195	0.60

[a] τ duration of hydrothermal treatment.
[b] from particle size distribution according to TEM (Fig. S2).

All obtained HB and CB-1 materials in Na-form were washed with distilled water, dried at 100 °C and calcined in air at 550 °C for 5 h (the heating rate was 2 °C/min). After calcination the samples were subjected two times to ion-exchange in 1 M NH_4Cl solution at 40 °C for 24 h to obtain NH_4^+-forms, which were then converted to the proton forms by calcination (heating to 550 °C with the ramp of 2 °C/min, holding time 5 h).

2.2 Characterization of catalysts

The phase composition of the obtained materials was analyzed using X-ray diffractometer D8 ADVANCE (Bruker AXS) with CuK_α-radiation. According to the technique reported previously [27], the degree of crystallinity (α_{cryst}) was evaluated by a change in the ratio of the area under the peak in the 2θ = 20 – 24° range in the XRD pattern of the investigated samples. For HB-2 material with the largest area in this range, the degree of crystallinity was accepted as unity.

The content of Si and Al was determined by energy dispersive X-ray spectroscopy using MIRA-3 instrument.

SEM images were obtained using the field emission SEM MIRA-3 (Tescan). Images were recorded using an accelerating voltage of 1 – 30 kV and a secondary electron detector. A sample

was loaded on the conductive graphitized support and recording was carried out without a preliminary deposition of conductive materials on the sample surface.

TEM images were obtained using field emission TEM JEM-2100F (JEOL) with an accelerating voltage of 200 kV. A sample was dispersed in ethanol in an ultrasonic bath for 5 min, and then the suspension was deposited to a copper grid coated with a carbon film.

Nitrogen adsorption was measured by the volumetric method (–196 °C, up to 1 atm) on the analyzer of porous materials Sorptomatic 1990 (Thermo Electron Corp.). Prior to measurements the samples were evacuated ($P \leq 0.7$ Pa) at 350 °C for 5 h. The specific surface area S_{BET} was evaluated by the BET equation [28]; the size of micropores was calculated by the method of Saito-Foley [29]; the size of mesopores was determined from the desorption branch of the isotherm, using the Barret-Joyner-Hallenda (BJH) method [30]. The micropore and mesopore volumes as well as the mesopore surface area (including the external surface area) were determined by the comparative *t*-plot method [31]. Argon adsorption was also measured by the volumetric method (–186 °C, up to 1 atm) on the same device. NLDFT pore size distribution curves [32] obtained from the argon ad(de)sorption isotherms on beta sample.

The acidic properties of the catalysts were investigated by temperature-programmed desorption of ammonia (TPDA) [33]. A sample was activated for 30 min in a flow of helium at 550 °C with the heating rate to a given temperature of 15 °C/min, cooled to 100 °C and saturated with ammonia for 20 min. Physically bound NH_3 was desorbed by purging with helium at 100 °C. The residual NH_3 was desorbed by heating in the temperature range of 100 – 700 °C (15 °C/min) and the positions of the desorption maxima were determined using a gas chromatograph LHM-80 equipped with a thermal conductivity detector and recorded as a TPDA curve. The total amount of desorbed ammonia was determined by titrating with $1 \cdot 10^{-3}$ M hydrochloric acid solution using an automatic titrating burette. The peak positions of thermal desorption of NH_3 were determined by deconvolution of TPDA curves using the Gaussian-type peak shape.

The method of pyridine ad(de)sorption with IR analysis widely applied for zeolites was used for characterization of the nature, strength and the total (in micropores and on mesopore surface) concentration of acid sites [34]. Thin wafers of the studied samples (8 – 12 mg/cm^2, without a binder) were placed in a cuvette with NaCl windows and evacuated (P = 1.4 Pa) at 400 °C for 1 h. Pyridine was adsorbed at 150 °C (in a cuvette with a sample) for 15 min, and desorbed at 150 – 400 °C (step 50 °C, holding time 30 min). Spectra of adsorbed pyridine were recorded using a Fourier spectrometer Spectrum One (Perkin Elmer). The concentration of Lewis (L-sites) and Brønsted (B-sites) acid sites was determined from the integral intensity of the absorption bands at 1454 cm^{-1} and 1545 cm^{-1} respectively using the integral molar absorption coefficients for these bands: ε(L) = 2.22 cm/μmol and ε(B) = 1.67 cm/μmol [35].

The method of 2,4,6-tri-*tert*-butylpyridine (TTBPy) ad(de)sorption with IR analysis [36] was used to study accessibility of the Brønsted acid sites for bulk molecules. The experimental technique is similar to the method described above for pyridine ad(de)sorption. 2,4,6-*Tri*-tert-butylpyridine was adsorbed at 150 °C for 1 h. The concentration of and Brønsted (B-sites) acid sites accessible for TTBPy was determined from the integral intensity of the absorption bands at 3370 cm^{-1} using the integral molar absorption coefficients for these band: ε(B) = 5.74 cm/μmol [37].

2.3 Catalytic tests

The Prins cyclization of (−)-isopulegol over synthesized hierarchical beta zeolites as well as with a conventional beta zeolite was performed in the liquid phase using a batch-mode operating glass reactor. (−)-Isopulegol (Sigma Aldrich, 98.9%) was used as received without further treatment. In a typical catalytic experiment, the initial concentration of (−)-isopulegol, the catalyst mass and the stirring speed were 0.013 mol/l, 50 mg and 375 rpm, respectively. The reaction conditions were selected to exclude mass transfer limitations.

Acetone (VWR Chemicals, 100%) was used as a reagent and a solvent (V = 50 ml), the reaction temperature was 30 °C. Prior to the reaction, the catalyst was dried overnight at 110 °C,

then treated in the reactor at 250 °C under an inert argon atmosphere for 30 min to remove moisture. The samples were taken at different time intervals and analyzed by GC. The products were confirmed by GC–MS (Agilent Technologies 6890 N). The samples were analyzed with a gas chromatograph (HP 6890) using HP-5 column (30 m, 320 μm, 0.50 μm) applying the following temperature programme: 100 °C (5 min) – 10 °C/min – 280 °C (10 min). The reactant and chromenols as well as dehydration products were calibrated using the standards prepared in Novosibirsk Institute of Organic Chemistry.

The number of the converted reactant molecules per total acid sites per unit time (h) (*i. e.* initial turnover frequency, 'TOF_{ini}') and 'total number of the reactant molecules converted per acid sites' during 4 h (*i. e.* turnover number, 'TON_{4h}') were calculated based on the total concentration of both Brønsted and Lewis acid sites accessible for pyridine molecules.

3. Results and discussion

3.1. Characterization results

Synthesized hierarchical zeolites HB-1 – HB-6 consist of fused beta zeolite nanoparticles with a size of 20 – 80 nm (according to XRD, TEM and SEM data, Figs. 2, 3 and Fig. S1 – S3, Table 1).

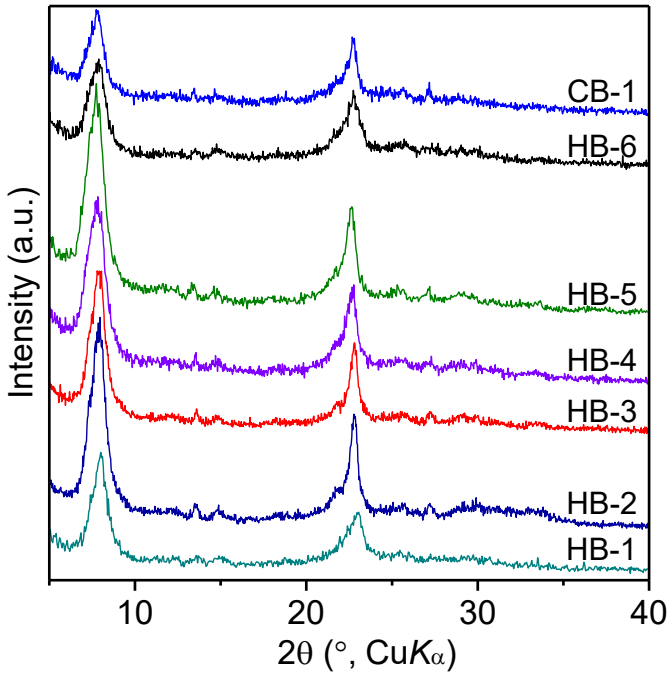

Fig. 2. XRD patterns of the calcined HB-1 – HB-6 and CB-1 catalysts.

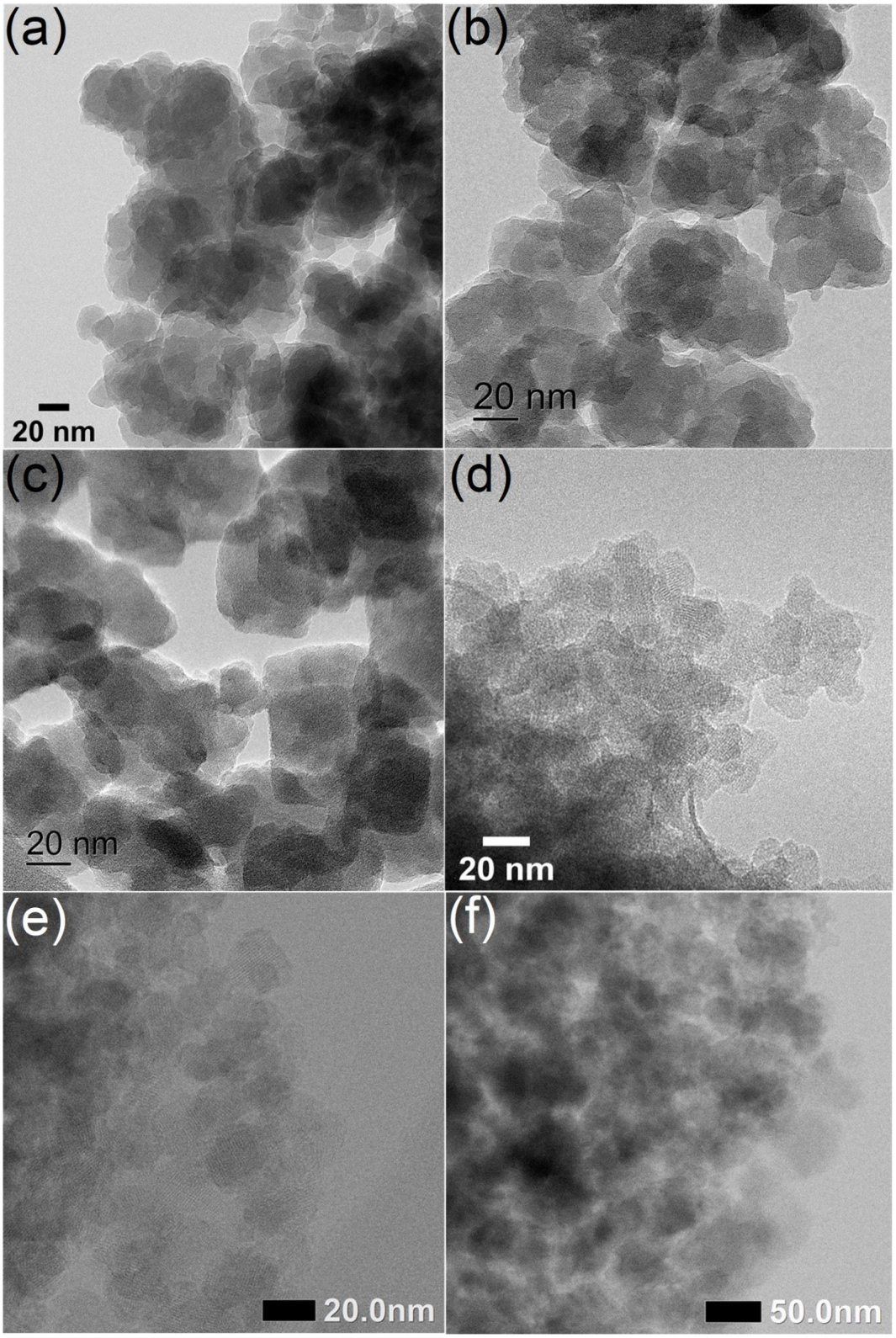

Fig. 3. TEM images of the calcined HB-1 (a), HB-2 (b), HB-3 (c), HB-4 (d), HB-5 (e) and HB-6 (f) materials.

The hydrothermal treatment of the RM with H_2O/Si = 2.5 at 140 °C for 2 day leads to formation of a partially crystalline material (HB-1, Figs. 2 and S1, Table 1), possessing beta zeolite nanoparticles with a size of 56 nm (according to TEM data, Figs. 3 and S2). An increase in the duration of HTT at 140 °C to 7 days results in an increase in the degree of crystallinity of the aluminosilicate (Table 1, sample HB-2). The particle size of HB-2 (45 nm) is significantly lower than that of beta zeolite CB-1 (ca. 0.2 μm, Figs. S4 and S5) obtained using diluted RM (H_2O/Si = 20). In concentrated RM a large number of zeolite nuclei is rapidly formed with a subsequent growth, crystallization and formation of a material consisting of zeolite nanoparticles agglomerates [38]. The sample HB-2 obtained in concentrated mixture is also characterized by the higher crystallinity in comparison with CB-1 (Table 1). A further increase in the duration of HTT to 9 days leads to the growth of zeolite nanoparticles up to 80 nm (HB-3 material, Figs. 3 and S2). Thus, with an increase in the duration of HTT of the RM with H_2O/Si = 2.5 from 2 days to 7 days the amorphous phase gradually crystallizes with the formation of beta zeolite nanoparticles. Prolongation of HTT to 9 days leads to an increase in the particles size as well as some decrease in the crystallinity of the materials due to the partial dissolution of the crystalline phase at increased duration of HTT of the highly alkaline concentrated mixture. The sample HB-4 obtained by HTT of the RM with H_2O/Si = 5.5 at 140 °C for 7 day contains beta zeolite nanoparticles with a size of 20 nm (Figs. 3 and S2). An increase in the H_2O/Si ratio to 7.0 leads to an increase in the zeolite crystallite size to 23 nm (sample HB-5, Table 1) and a certain increase in α_{cryst}. Prolongation of HTT of the RM with H_2O/Si = 5.5 at 140 °C to 9 days results in a growth of zeolite nanoparticles up to 44 nm (sample HB-6, Table 1, Fig. S2) and a decrease in the degree of crystallinity also due to the dissolution of crystalline phase.

Nitrogen ad(de)sorption isotherms (–196 °C) for HB-1 – HB-6 (Fig. 4) can be assigned to type IV (according to IUPAC classification) with the adsorbate uptake at p/p_0 <0.1 and the hysteresis loop at 0.7 – 0.97 corresponding to micropore filling with N_2 and its condensation in interparticle mesopores, respectively. The isotherm of CB-1 is referred to type I with only a small

adsorbate uptake at p/p_0 >0.1. The porous system of HB-1 – HB-6 includes micropores (V_{micro} = 0.21 – 0.25 cm^3/g, D_{micro} = 0.65 nm, Table 2) and in contrast to CB-1, the interparticle voids of mesopore size (V_{meso} = 0.43 – 0.84 cm^3/g, S_{meso} = 85 – 230 m^2/g, D_{meso} = 15.4 – 36.1 nm) (Fig. 4). The micropore and mesopore size distribution curves (NLDFT, argon adsorption at –186 °C) for HB-4 (the average diameter of micropores 0.62 nm and mesopores 15.5 nm) are shown in Fig. S6.

Table 2

Characteristics of the porous structure (N_2, –196 °C) of the obtained materials

Sample	V_{micro}[a] (cm^3/g)	V_{meso}[b] (cm^3/g)	D_{meso}[c] (nm)	S_{meso}[d] (m^2/g)	S_{BET}[e] (m^2/g)
HB-1	0.24[f]	0.43	50±7.4	110	670
HB-2	0.25	0.69	36±15.3	130	760
HB-3	0.23	0.46	–[g]	85	640
HB-4	0.21	0.81	15±0.9	230	765
HB-5	0.23	0.84	19±1.5	200	780
HB-6	0.24	0.65	30±11.8	105	670
CB-1	0.20	0.15	–	40[h]	520

[a] V_{micro}, micropore volume.
[b] V_{meso}, mesopore volume.
[c] D_{meso}, mesopore diameter. Gaussian distribution (standard deviation) is used to estimate the error in the mesopore diameter.
[d] S_{meso}, mesopore surface area.
[e] S_{BET}, total specific surface area.
[f] Micropore diameter for the samples given in Table 2 is 0.65 nm.
[g] Mesopore size distribution without a maximum.
[h] The external surface area of beta zeolite.

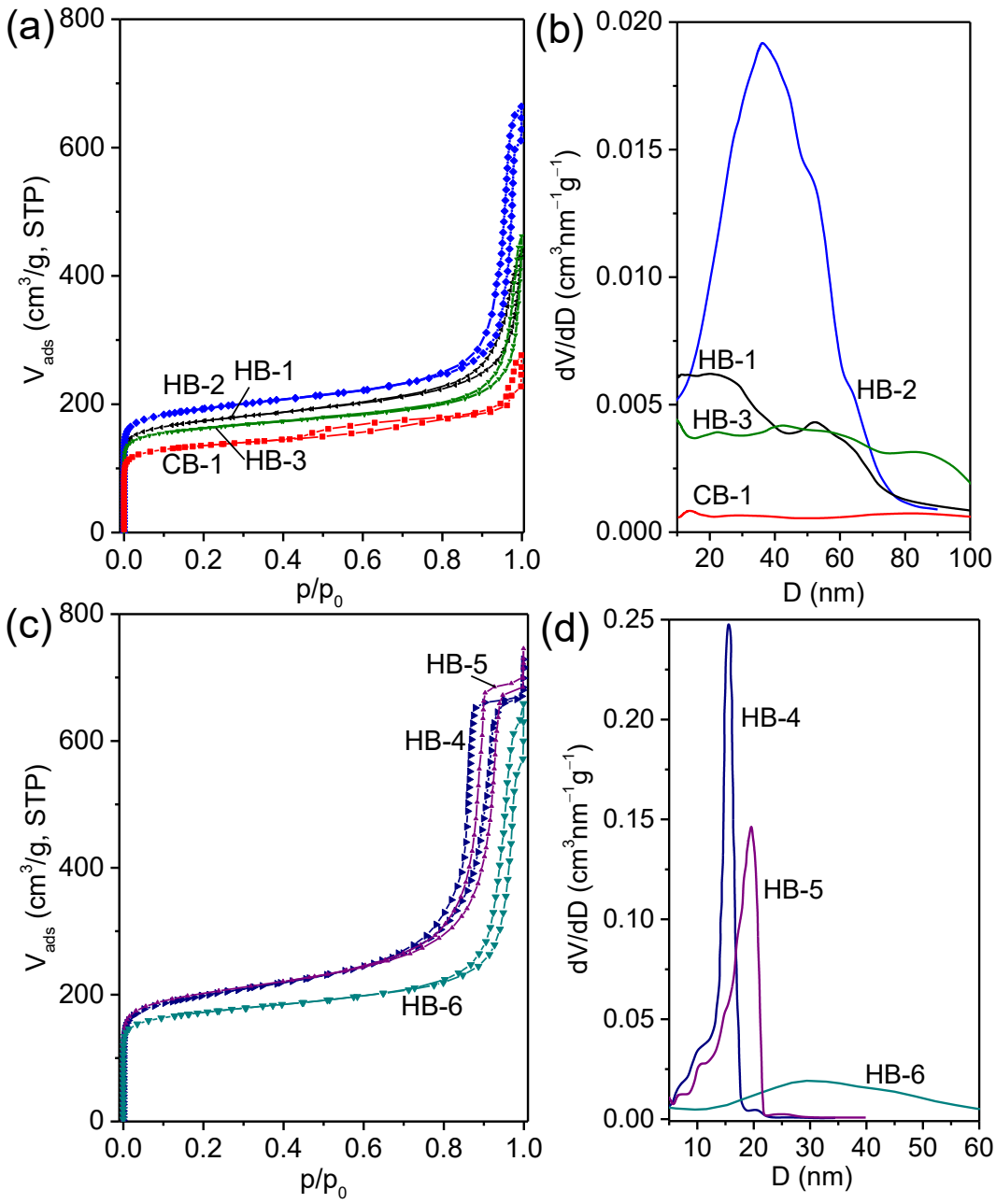

Fig. 4. Nitrogen ad(de)sorption isotherms at –196 °C (a), (c) and mesopore size distribution (from the desorption branch) curves (b), (d) for HB-1 – HB-6 and CB-1 materials.

An increase in the duration of HTT at 140 °C from 2 to 7 days results in an increase in the mesopore volume and the surface area, S_{BET} (Table 2) as could be anticipated. For HB-3 material, a rise in the nanoparticles size leads to a decrease in the parameters of its porous structure (Table 2). An increase in the mesopore volume (up to 0.81 cm^3/g) and the surface area (up to 230 m^2/g), as well as mesopore size uniformity (D_{meso} = 15±0.9 nm, Fig. 4) was observed with elevation of the

H_2O/Si ratio in the gel from 2.5 (HB-2) to 5.5 (HB-4). A further increase from 5.5 to 7.0 (HB-5) results in a decrease in the mesopore surface area (Table 2), as well as the mesopore broadening from 15.4 to 19.4 nm (Fig. 4). TEM images (Fig. 3) of calcined HB-4 and HB-5 materials also confirm the presence of interparticle mesopores with a uniform size (ca. 20 nm). Obviously, an optimal balance is reached between the dissolution and crystallization rates at the H_2O/Si ratio of 5.5 and the corresponding alkalinity [39], which allows synthesis of a highly porous material formed by small zeolite nanoparticles (15 nm). For HB-6 material, an increase in the nanoparticles size is accompanied by a decrease in the mesopore volume and the surface area (Table 2).

The acidic properties of the obtained catalysts HB-1 – HB-6 were characterized by TPDA and FTIR with pyridine ad(de)sorption. According to TPDA data (Table 3) HB-1 – HB-6 materials with the Si/Al ratio of 19 – 27, as well as CB-1 (Si/Al = 20), contain medium and strong acid sites with NH_3 desorption maximum at 335 – 370 °C. HB-2 and HB-3 materials obtained by HTT of the RM at 140 °C for 7 and 9 days respectively are characterized by a higher concentration of acid sites (Table 3) in comparison with HB-1 (HTT for 2 days), which can be related to a higher degree of crystallinity of HB-2 and HB-3 (Table 1). The concentration of acid sites of the samples HB-4 and HB-5 (245 – 295 μmol/g) exceeds the corresponding value for HB-6 (179 μmol/g), which can also be associated with a difference in α_{cryst} of the samples.

According to the FTIR data of pyridine ad(de)sorption, HB-2 and HB-3 materials are characterized by a higher total concentration of medium and strong Brønsted acid sites (Table 4), as well as the ratio between Brønsted and Lewis acid sites (2.1) in comparison with HB-1 (C_B/C_L = 1.5). This is related to an increase in α_{cryst} with prolongation of HTT of the RM at 140 °C from 2 to 7 – 9 days. HB-4 and HB-5 with the degree of crystallinity of 0.85 – 1.0 are characterized by a larger proportion of strong Brønsted acid sites (0.46) compared to HB-6 with α_{cryst} of 0.60 (0.40).

FTIR of 2,4,6-*tri*-tert-butylpyridine (TTBPy) ad(de)sorption was used for estimation of the accessibility of Brønsted acid sites for the bulk molecules which are larger than the micropore size of beta zeolite. 2,4,6-Tri-tert-butylpiridine can interact only with the Brønsted acid sites located on

the external or mesopore surfaces because the cross section of the molecule is too large to enter 12-MR pores of beta zeolites. The concentration of Brønsted acid sites calculated using integral intensities of the absorption band at 3370 cm^{-1} corresponding to the vibrations of $\equiv N–H^+$ of protonated TTBPy for HB-1 – HB-6 materials is 2.1 – 4.6 fold higher than those of CB-1 (Table 5) with a small external surface area (40 m^2/g). The sample HB-2 with the degree of crystallinity α_{cryst} = 1.0 is characterized by a larger contribution of strong Brønsted acid sites on the mesopore surface (0.70) compared to other hierarchical beta materials (0.50 – 0.55).

Table 3

Si/Al molar ratio in the catalysts and their acidity by temperature-programmed desorption of ammonia.

Sample	Si/Al	Acidity by TPDA	
		T_{max}[a] (°C)	C[b] (μmol/g)
HB-1	27	220	94
		355	133
HB-2	31	200	178
		355	251
HB-3	29	200	137
		340	240
HB-4	26	200	205
		335	295
HB-5	19	190	378
		345	245
HB-6	27	200	48
		345	179
CB-1	20	215	127
		370	303

[a] T_{max}, temperature of the maximum of ammonia desorption.
[b] C, concentration of acid sites.

Table 4

Acidity of the catalysts by FTIR with pyridine ad(de)sorption.

Sample	Brønsted acid sites concentration (μmol/g)				Lewis acid sites concentration (μmol/g)	Total acid sites concentration (μmol/g)
	Week[a]	Medium	Strong	Total		
HB-1	35	37	35	107	73	180
HB-2	36	40	48	124	62	186
HB-3	28	38	37	103	49	152
HB-4	37	38	63	138	64	202
HB-5	25	36	53	114	53	167
HB-6	32	36	48	115	55	170
CB-1	28	38	65	131	52	183

[a] Week acid sites – pyridine is desorbed in the range of 150 – 250 °C, medium acid sites – pyridine is desorbed in the range of 250 – 350 °C, strong acid sites – pyridine remains after desorption at 350 °C.

Table 5

Acidity of the catalysts by FTIR with 2,4,6-tri-*tert*-butylpyridine ad(de)sorption.

Sample	Brønsted acid sites concentration (μmol/g)			
	Week[a]	Medium	Strong	Total
HB-1	6	9	14	29
HB-2	2	6	19	27
HB-3	6	11	19	36
HB-4	10	15	30	55
HB-5	11	16	33	60
HB-6	6	10	18	34
CB-1	1	3	9	13

[a] Week acid sites – TTBPy is desorbed in the range of 150 – 250 °C, medium acid sites – TTBPy is desorbed in the range of 250 – 350 °C, strong acid sites – TTBPy remains after desorption at 350 °C.

3.2 Catalytic activity

The prepared hierarchical beta zeolites were investigated in the Prins cyclization between (–)-isopulegol and acetone (Table 6).

Table 6

Catalytic results for hierarchical beta zeolites in Prins cyclization between (–)-isopulegol and acetone.

Catalyst	Initial reaction rate (mmol/min g_{cat})	Conversion of (–)-isopulegol after 4 h (%)	Yield of chromenols R+S after 4 h (%)	R/S ratio at 30% conversion (%)[a]	Selectivity to R+S chromenols at 30% conversion (%)[a]	Selectivity to dehydration products at 30% conversion (%)
HB-1	0.2	44.7	30.6	10.6 (10.5)	67.4 (68.5)	32.6 (31.5)
HB-2	0	47.1	31.1	11.2 (11.1)	64.3 (66.0)	35.7 (34.0)
HB-3	3.4	34.7	21.3	8.5 (8.5)	48.0 (61.4)	52.0 (38.6)
HB-4	1.0	51.8	33.8	10.9 (10.8)	63.2 (65.2)	36.8 (34.8)
HB-5	2.2	38.0	24.8	10.0 (10.0)	61.8 (65.2)	38.2 (34.8)
HB-6	1.6	30.1	20.1	9.5 (9.5)	66.8 (66.8)	33.2 (33.2)
CB-1	2.5	38.6	25.5	9.9 (9.9)	62.2 (66.1)	37.8 (33.9)

[a] In parenthesis after 4 h.

A comparison of isopulegol conversion over different catalysts showed that mesoporous beta zeolite HB-4 demonstrated the highest conversion of IP (ca. 52%, Fig. 5). Furthermore, it can be clearly seen from Fig. 5 that the activity of HB-1, HB-2 and HB-4 remained high after prolonged reaction times, while activity of other catalysts declined after 30 min. HB-5 exhibited very high acidity according to ammonia TPD resulting in catalyst deactivation. At the same time CB-1 contained just a small amount of mesopores, while micropores present in this catalyst are more prone to deactivation by pore blocking.

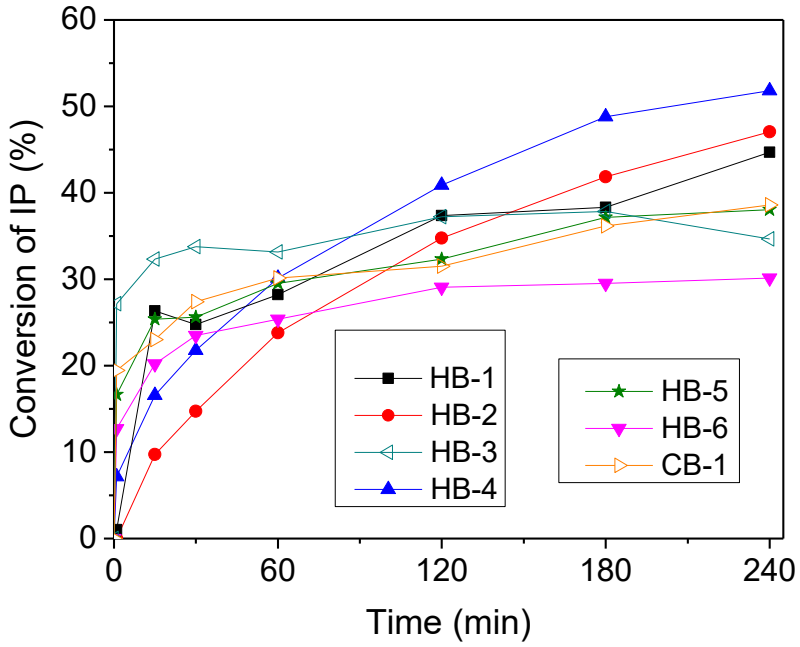

Fig. 5. Conversion of (−)-isopulegol (IP) as a function of the reaction time over hierarchical beta zeolites.

The highest yield of chromenols was obtained over HB-4 catalyst, (ca. 34%) within 240 min from the beginning of the reaction. The highest catalytic activity of HB-4 can be connected with the developed mesoporosity and high concentration of Brønsted acid sites accessible for TTBPy (55 μmol/g) characterized by the most uniform mesopore size (D_{meso} = 15±0.9 nm, Fig. 4) among the studied materials. HB-6 exhibited the lowest conversion of IP (ca. 30%) leading, respectively, to the lowest yield of the desired products (ca. 20%) which can be associated with lower mesopore volume and surface area connected to a larger nanoparticles size (40 – 50 nm) compared to other investigated catalysts. Other samples exhibit higher (HB-1 and HB-2) or similar (HB-3 and HB-5) conversion levels in comparison with a conventional beta zeolite CB-1 (ca. 39%).

The initial reaction rates were calculated according to

$$r_0 = \frac{(c_0 - c_t)\cdot V}{t}\frac{1}{m_{cat}} \quad (1)$$

where c_0, c_t are the initial and actual concentrations of isopulegol IP (mmol/l), V – reaction volume (l), t is a reaction time (1 min) and m_{cat} is the mass of catalyst (g). As can be seen from the

calculated data (Table 6) the reaction is characterized by a relatively low reaction rate without achieving complete conversion of (−)-isopulegol. The highest reaction rate was observed for HB-3 catalyst which, considering the lowest selectivity towards the desired chromenols, is characterized by much faster side dehydration reactions. As a result, HB-3 demonstrated the highest catalytic activity in terms of initial TOF values (Fig. 6a). HB-4 catalyst is the most active in terms of TON_{4h} values (Fig. 6b) which can be associated with the developed mesoporosity, a large fraction of strong Brønsted acid sites on the mesopore surface (Table 5) and high concentration of accessible acid sites (Table 4). The obtained low TON_{4h} values are obviously connected with the incomplete conversion of (−)-isopulegol.

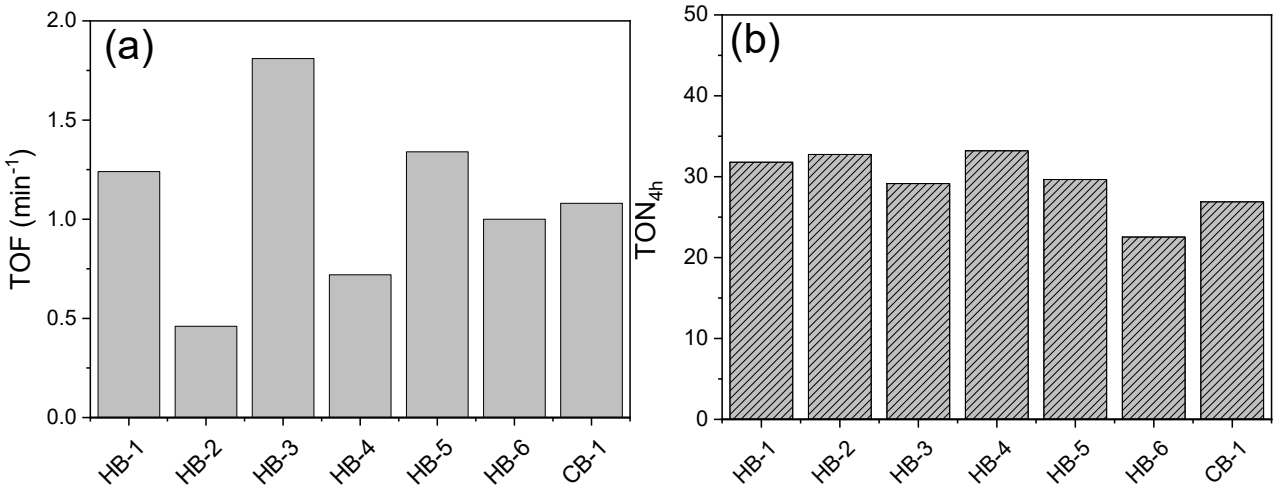

Fig. 6. Initial TOF (a) and TON after 4 h (b) obtained in the Prins cyclization between (–)-isopulegol and acetone over hierarchical beta zeolites. Calculations of TOF and TON correspond to 15 min and 4 h respectively.

Less efficient catalytic performance of the prepared hierarchical beta zeolites in the investigated Prins cyclization of (−)-isopulegol with acetone compared to a similar reaction between (−)-isopulegol and benzaldehyde even over less accessible ZSM-5 based catalysts [40] should be noted. This behavior is obviously related to a higher reactivity of a primary carbonyl group in benzaldehyde compared to a keto group in acetone.

Dependences of the catalytic activity of hierarchical beta zeolites on the concentrations of Brønsted and Lewis acid sites indicate a certain increase of the reagent conversion and *R/S* chromenols ratio with an increase in the concentration of corresponding acid sites (Fig. 7a). 4*R* to 4*S* isomer ratio is an important characteristic due to the antiviral properties inherent only to 4*R* chromenol and should be considered during evaluation of the efficiency of catalysts in the Prins cyclization. More clear correlations can be seen for total acidity (Fig. 7b).

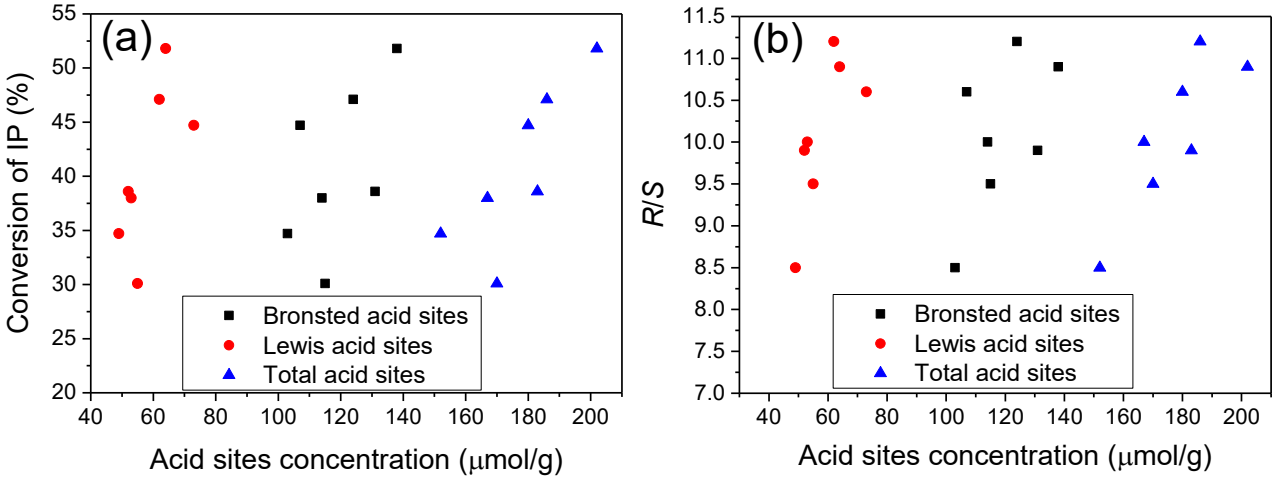

Fig. 7. Conversion of (−)-isopulegol (a) and *R/S* chromenols ratio (b) as a function of acid sites concentration.

It should be pointed out that the prepared zeolite catalysts allowed a high 4*R* and 4*S* diastereoisomers ratio (R/S ratio, up to 11.2, Table 6) which is higher than previously reported for halloysite nanotubes (HNT) pretreated with HCl [13]. In addition, no isopulegol-chromenol ether (compound **6** in Fig. 1) was formed.

Selectivity towards the desired *R* chromenol (4*R* diastereoisomer of chromenol) practically does not depend on the ratio of Brønsted to Lewis acid sites (Fig. 8, the lower point can be considered as an outlier) which can indicate the key role of the steric factors rather than acidity in the studied reaction.

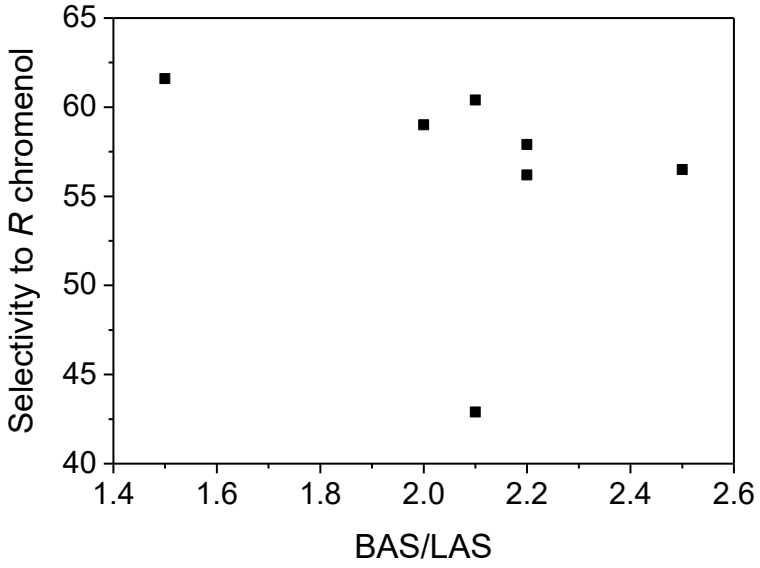

Fig. 8. Selectivity towards *R* chromenol at 30% conversion as a function of the ratio of Brønsted and Lewis acid sites.

Quantum chemical calculations of the stability of the reaction products [14] showed only a slightly higher Gibbs free energy for the *S*- compared to the *R*-diastereomer. Subsequently it was concluded that the reagents adsorption mode and the reaction kinetics have a major impact on the *R/S* ratio rather than thermodynamics. Small differences between the Gibbs energies of the isomers probably point on steric limitations during formation of the *S*-product [14]. Obviously the hierarchical structure of the prepared zeolites allows to avoid catalyst deactivation by the pore blocking considering a relatively large size of the reaction products. Moreover, generation of mesoporosity in the zeolite structure results in a significant increase of the concentration of accessible Brønsted acid sites (Table 5) which were found to be responsible for formation of the desired products [14].

For further elucidation of the reaction mechanism, the concentrations of dehydration products were plotted against the concentration of chromenols (Fig. 9). Figure 9 illustrates that the yields of chromenols were much lower over zeolites than over a sulphonic acid modified clay, K-CSA-10 [14]. The origin for lower conversion levels over zeolites might be the presence of water formed via dehydration. The total yields of chromenols were for HB-4 and K10-CSA 33.8% and 83%

respectively [14]. The highest conversion was obtained over strongly Brønsted acidic catalyst K10-CSA[14], in which no Lewis acid sites were present. From the kinetic data it can be stated that formation of dehydration products and chromenols occurred in a parallel fashion.

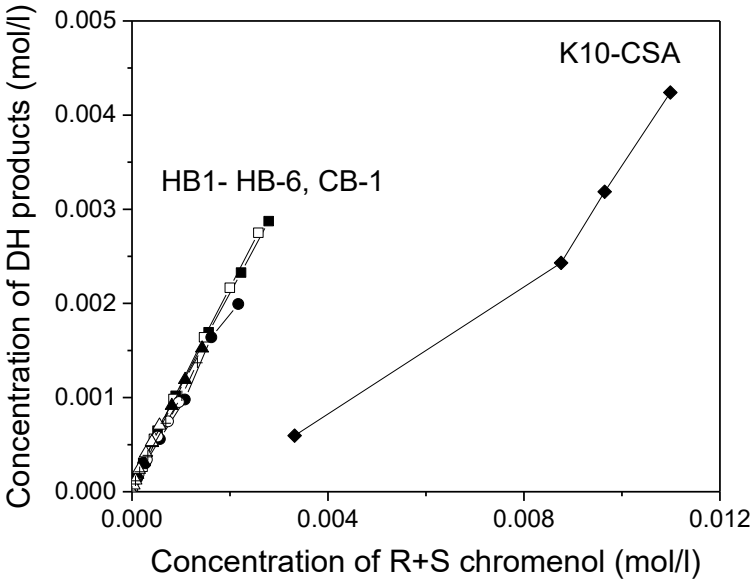

Fig. 9. Concentration of dehydration products vs chromenols over different hierarchical zeolites in this study and sulphonic acid modified clay K10-CSA obtained in Prins cyclization between (-)-isopulegol and acetone at 30 °C[14].

The mechanistic pathway of the cyclization reaction using (−)-isopulegol and acetone previously proposed in [14] includes protonation of the carbonyl group of acetone followed by the attack by the OH-group of (−)-isopulegol, the proton transfer and water removal resulting in the formation of oxocarbenium ion. The last one is attacked by C=C double bond leading to the carbocation which further reacts with a corresponding nucleophile producing the desired product **4R/4S** (Fig.1, molar mass of 212 g/mol). The side products (olefins in Fig. 1) can be generated via the proton elimination from the carbocation or chromenols dehydration [14].

Dehydration of the chromenol product in a diastereo-selective fashion was previously considered for the Prins addition of isopulegol with thiophene-2-carbaldehyde [13]. In the current case the data on the 4R/4S ratio as a function of conversion (Fig.10) indicate that this ratio is constant, subsequently the diastereo-selective elimination of water from 4R-chromenol product to

the dehydration products can be neglected contrary to our previous work with thiophene-2-carbaldehyde [13]. Moreover, a high 4*R*/ 4*S* ratio almost independent on the ratio of Brønsted to Lewis acid sites points out also on the key role of the steric factors rather than acidity in the studied reaction or water as the nucleophile. In the reference [13], potential steric restrictions in diastereoselection were discussed for thiophene-2-carbaldehyde addition to isopulegol, where it was suggested that the adsorption mode comprising interactions of the S atom with the surface of the halloysite is preferred over the one where such interactions are absent. As a result mainly the 4R product was formed. Apparently, a similar analysis invoking calculations of the energy profiles for 4R and 4S diastereomers on the zeolites in required to explain the reason of preferential 4R diastereomer formation.

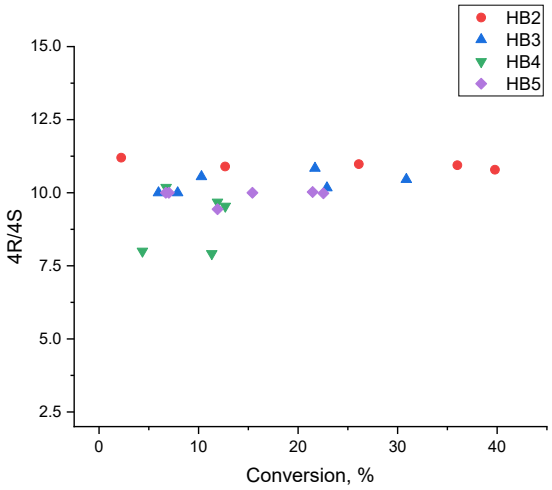

Figure 10. The 4R/4S ratio as a function of conversion for different hierarchical zeolites.

The ratio between the initial rates for formation of dehydration products vs chromenols, $r_{0,DH}/r_{0,chr}$ increased in the following order: 0.18 (K10-CSA) < 1.29 (zeolite catalysts) indicating that the most selective catalyst for chromenols was K10-CSA followed by zeolites.

For the most active catalyst (HB-4) a filtrate test was carried out as follows: the reaction was started in the presence of the catalyst, which was filtrated away at 9 min and the reaction was continued without the catalyst after 60 min in the reactor under stirring. The results demonstrated

that acid sites were not leached into the liquid phase, i.e. a possible homogeneous reaction did not occur (Fig. 11a), because (−)-isopulegol was not converting further without a catalyst. In order to check repeatability of the experimental procedure, two experiments were performed with a fresh HB-4 catalyst with the results showing excellent repeatability (Fig. 11b). Moreover, the catalyst structure stability was confirmed by the XRD data of the initial and spent samples (Fig. S7). The obtained identical XRD patterns testify stable both phase composition and particle size of the catalyst.

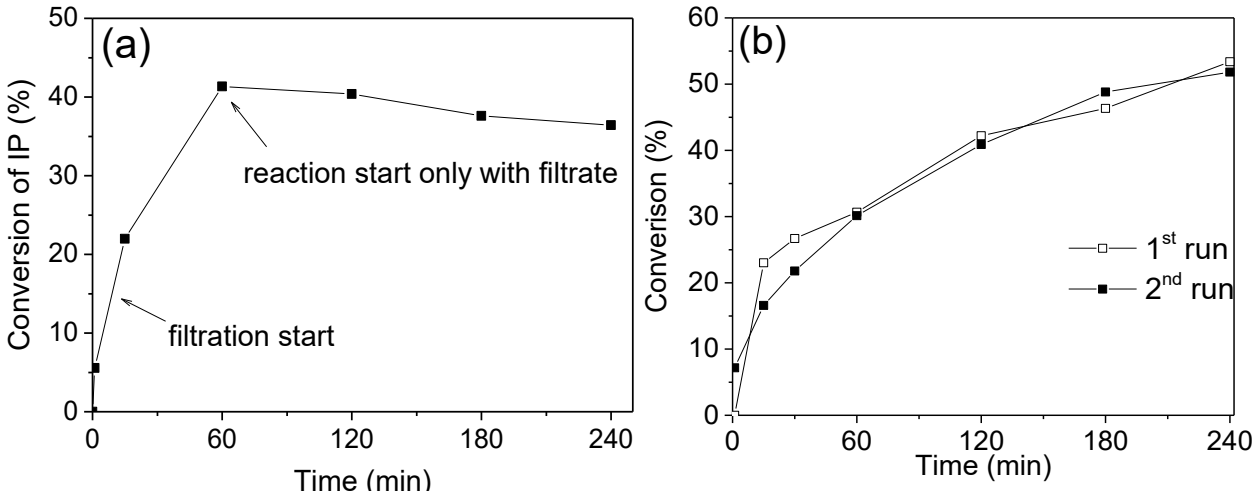

Fig. 11**.** Filtration (a) and repeatability (b) test using HB-4 in Prins cyclization of (−)-isopulegol with acetone

A possible reason for a lower catalytic activity of the prepared hierarchical zeolites compared to K10-clay modified by sulfonic acid [14] is the fact that a certain part of catalytically active sites is located inside the micropores and can be inaccessible for the reactants. Therefore, a lower micropore content in hierarchical zeolites or application of micro-mesoporous zeolite materials without micropores can be one of the ways for further improvement of catalytic performance of zeolite based catalysts. However, the obtained results can be considered very promising due to much higher R/S ratio for micro-mesoporous zeolites than for clays and well-known excellent stability of zeolites. Moreover, a tendency of sulphonic groups leaching from K10 clay and similar functionalized materials is an obvious drawback limiting their application in catalysis.

Conclusions

Hierarchical beta zeolites obtained via hydrothermal treatment of a concentrated zeolite gel-precursor were investigated in Prins cyclisation between (-)-isopulegol and acetone under mild conditions (30 °C). The highest yield of the desired chromenols, exhibiting antiviral properties, was reached over HB-4 zeolite consisting of fused beta zeolite nanoparticles with a small size (15 nm) which resulted in the formation of the developed mesoporous structure (V_{meso} 0.81 cm^3/g, S_{meso} 230 m^2/g) with the increased concentration of highly-accessible Brønsted acid sites and highest mesopore size uniformity (D_{meso} = 15±0.9 nm) among the studied zeolite materials. Application of the prepared zeolite catalysts allowed a high 4*R* to 4*S* diastereoisomers ratio (up to 11.2) exceeding previously reported in the literature.

Acknowledgement

NS acknowledges the support of the National Research Foundation of Ukraine to the project "New effective zeolite catalysts for environmentally friendly processes of the conversion of renewable raw materials into valuable organic compounds" (project number 2020.02/0335). RB acknowledges the support of the Czech Science Foundation to the project EXPRO (19-27551X).

The authors express their gratitude to colleagues from L.V. Pisarzhevsky Institute of Physical Chemistry who contributed to the experimental part, in particular Pavel Yaremov for nitrogen adsorption measurements and Valentina Tsyrina for TPD of ammonia. The authors acknowledge the contribution of Dr. Igor Bezverkhyy (Université de Bourgogne, France), Dr. Mykola Skoryk ("NanoMedTech", Ukraine), Dr. Sergii Sergiienko (University of Aveiro, Portugal), Kateryna Filatova (Tomas Bata University in Zlín, Czech Republic) and Ang Li (Charles University in Prague) in carrying out SEM and TEM investigations.

References

[1] R.A. Sheldon, Green Chem. 16 (2004) 950–963.

[2] P. Marion, B. Bernela, A. Piccirilli, B. Estrine, N. Patouillard, J. Guilbot, F. Jérôme, Green Chem. 19 (2017) 4973–4989.

[3] R. Pratap, V.J. Ram, Chem. Rev. 114 (2014) 10476–10526.

[4] N. Majumdar, N.D. Paul, S. Mandal, B. de Bruin, W.D. Wulff, ACS Catal. 5 (2015) 2329–2366.

[5] E. Nazimova, A. Pavlova, O. Mikhalchenko, I. Il'ina, D. Korchagina, T. Tolstikova, K. Volcho, N. Salakhutdinov, Med. Chem. Res. 25 (2016) 1369–1383.

[6] M. Stekrova, P. Mäki-Arvela, N. Kumar, E. Behvaresh, A. Aho, Q.Balme, K.P. Volcho, N.F. Salakhutdinov, D.Yu. Murzin, J. Mol. Catal. A 410 (2015) 260–270.

[7] M.N. Timofeeva, K.P. Volcho, O.S. Mikhalchenko, V.N. Panchenko, V.V. Krupskaya, S.V. Tsybulya, A. Gil, M.A. Vicente, N.F. Salakhutdinov, J. Mol. Cat. A Chem. 398 (2015) 26–34.

[8] M.N. Timofeeva, V.N. Panchenko, K.P. Volcho, S.V. Zakusin, V.V. Krupskaya, A. Gil, O.S. Mikhalchenko, J. Mol. Catal. A 414 (2016) 160–166.

[9] G. Baishya, B. Sarmah, N. Hazarika, Synlett 24 (2013) 1137–1141.

[10] N. Li-Zhulanov, P. Mäki-Arvela, M. Lulac, A.F. Peixoto, E. Kholkina, A. Aho, K. Volcho, N. Salakhutdinov, C. Freire. A.Yu. Sidorenko, D.Yu. Murzin, Mol. Catal. 478 (2019); 110569

[11] I.V. Ilyina, V.V. Zarubaev, I.N. Lavrentina, A.A. Shtro, I.L. Esaulkova, D.V. Korchagina, S.S. Borisevich, K.P. Volcho, N.F. Salakhutdinov, Bioorg. Med. Chem. Lett. 28 (2018) 2061–2067.

[12] K.R. Kishore, K. Reddy, L.F. Silva Jr., J. Braz. Chem. Soc. 24 (2013) 1414–1419.

[13] A.Yu. Sidorenko, A.V. Kravtsova, I.V. Il'ina, J. Wärnå, D.V. Korchagina, Yu.V. Gatilov, H. Pazniak, K.P. Volcho, N.F. Salakhutdinov, D.Yu. Murzin, V.E. Agabekov, J. Catal. 380 (2019) 145–152.

[14] M. Laluc, P. Mäki-Arvela, A. F. Peixoto, N. Li-Zhulanov, T. Sandberg, N. F. Salakhutdinov, K. Volcho, C. Freire, A. Yu. Sidorenko, D. Yu. Murzin, React. Kinet. Mech. Catal. 129 (2020) 627–644.

[15] J. Čejka, R. Millini, M. Opanasenko, D.P. Serrano, W.J. Roth, Catal. Today. 345 (2020) 2–13.

[16] L.-H. Chen, M.-H. Sun, Z. Wang, W. Yang, Z. Xie, B.-L. Su, Chem. Rev. 120 (2020) 11194–11294.

[17] P. Peng, X.H. Gao, Z.F. Yan, S. Mintova, Natl. Sci. Rev. 7 (2020) 1726–1742.

[18] B.S. Rana, B. Singh, R. Kumar, D. Verma, M.K. Bhunia, A. Bhaumik, A.K. Sinha, J. Mater. Chem., 20 (2010) 8575–8581.

[19] A.K. Patra, A. Dutta, M. Pramanik, M. Nandi, H. Uyama, A. Bhaumik, ChemCatChem, 6 (2014) 220–229.

[20] W. Schwieger, A.G. Machoke, T. Weissenberger, A. Inayat, T. Selvam, M. Klumpp, A. Inayat, Chem. Soc. Rev. 45 (2016) 3353–3376.

[21] D.P. Serrano, J.M. Escola, P. Pizarro, Chem. Soc. Rev. 42 (2013) 4004–4035.

[22] S. Mitchell, A.B. Pinar, J. Kenvin, P. Crivelli, J. Kärger, J. Pérez-Ramírez, Nat. Commun. 6 (2015) 8633–8646.

[23] W. Khan, X. Jia, Z. Wu, J. Choi, A.C.K. Yip, Catalysts 9 (2019) 127.

[24] J. Přech, P. Pizarro, D.P. Serrano, J. Čejka, Chem. Soc. Rev. 47 (2018) 8263–8306.

[25] Z. Liu, Y. Hua, J. Wang, X. Dong, Q. Tian, Y. Han, Mater. Chem. Front. 1 (2017) 2195–2212.

[26] R. Barakov, N. Shcherban, P. Yaremov, I. Bezverkhyy, V. Tsyrina, M. Opanasenko, Appl. Catal. A Gen. 594 (2020) 117380.

[27] M.A. Camblor, A. Corma, S. Valencia, Microporous Mesoporous Mater. 25 (1998) 59–74.

[28] S. Brunauer, P.H. Emmett, E. Teller, J. Am. Chem. Soc. 60 (1938) 309–319.

[29] A. Saito, H.C. Foley, AIChE J. 37 (1991) 429–436.

[30] E.P. Barrett, L.G. Joyner, P.P. Halenda, J. Am. Chem. Soc. 73 (1951) 373–380.

[31] B.C. Lippens, J.H. de Boer, J. Catal. 4 (1965) 319–323.

[32] M. Thommes, in: J. Čejka, H. van Bekkum, A. Corma, F. Schüth (Eds.), Introduction to Zeolite Science and Practice 3rd Revised Edition, Stud. Surf. Sci. Catal., vol. 168, Elsevier, Amsterdam, 2007, pp. 495–523.

[33] L.-E. Sandoval-Díaz, J.-A. González-Amaya, C.-A. Trujillo, Microporous Mesoporous Mater. 215 (2015) 229–243.

[34] K. Kim, R. Ryoo, H.D. Jang, M. Choi, J. Catal. 288 (2012) 115–123.

[35] C.A. Emeis, J. Catal. 141 (1993) 347–354.

[36] H.K. Heinichen, W.F. Hölderich. J Catal. 85 (1999) 408–414.

[37] L. Lakiss, A. Vicente, J.-P. Gilson, V. Valtchev, S. Mintova, A. Vimont, R. Bedard, S. Abdo, J. Bricker, ChemPhysChem 21 (2020) 1873–1881.

[38] K. Möller, B. Yilmaz, R.M. Jacubinas, U. Müller, T. Bein T, J. Am. Chem. Soc. 133 (2011) 5284–5295.

[39] K. Möller, B. Yilmaz, U. Müller, T. Bein T, Chem. - A Eur. J. 18 (2012) 7671–7674.

[40] E. Kholkina, P. Mäki-Arvela, C. Lozachmeuer, R. Barakov, N. Shcherban, D.Yu. Murzin, Chinese J. Catal. 40 (2019) 1713–1720.